ISSN 1069-3513, Izvestiya, Physics of the Solid Earth, 2012, Vol. 48, No. 1, pp. 42–60. © Pleiades Publishing, Ltd., 2012.
Original Russian Text © D.M. Pechersky, A.A. Lyubushin, Z.V. Sharonova, 2012, published in Fizika Zemli, 2012, No. 1, pp. 44–62.

On the Coherence between Changes in Biota and Geomagnetic Reversals in the Phanerozoic

D. M. Pechersky, A. A. Lyubushin, and Z. V. Sharonova

Institute of Physics of the Earth, Russian Academy of Sciences, ul. Bol'shaya Gruzinskaya 10, Moscow, 123995 Russia

Received May 5, 2010; in final form, August 2, 2010

Abstract—The data on geomagnetic reversals, organic changes, and lower-mantle plume magmatism in the Phanerozoic are collected and correlated. No direct relationship is revealed between the geomagnetic reversals, plumes, and biozones. However, the frequency of geomagnetic reversals is found to correlate to the frequency of biozonal alterations. We relate this inconsistency to the coupling of the two processes, which are mutually independent, with the long-term changes in the Earth's rotation. The plumes are formed at the core-mantle boundary and, thus, the reversals should have a different source. We hypothesize that the change in the geomagnetic polarity is due to the nonuniform rotation of the inner core relative to the mantle in combination with the changes in the axial tilt of the Earth's rotation.

Keywords: geomagnetic reversal, magnetochron, inner core of the Earth, biozone, biota, the Phanerozoic.

DOI: 10.1134/S1069351311120081

INTRODUCTION

In this work, we compare four types of processes: (1) those occurring exceptionally in the core of the Earth (variations and reversals of the geomagnetic field); (2) those originating at the core-mantle boundary, rising upwards, and reaching the surface of the Earth (the plumes); (3) those strictly confined to the Earth's surface (the changes in the organics); and (4) those synchronously involving the *whole* body of the planet (the Earth's rotation around its axis). Previously, we revealed the increase in the amplitude of directional geomagnetic variations on approaching the centers of the world magnetic anomalies and epicenters of the mantle plumes (Pechersky, 2001; 2007; 2009; Pechersky and Garbuzenko, 2005). This fact points to tight coupling between these factors, as all of them are generated by local disturbances at the core–mantle boundary (Grachev, 2000; Zharkov, Karpov, and Leont'ev, 1984; Ernst and Buchan, 2003, etc.).

When comparing geomagnetic reversals against a succession of stratigraphic stages, it was found that the stratigraphic boundaries do not correlate to the reversals while the rate of flips in geomagnetic polarity is synchronized with the rate of changes of stratigraphic stages (Pechersky, 2000; Pechersky, Lyubushin, and Sharonova, 2010). This feature is only recognizable with extensive averaging of the data over a period of 10 m.y., as the durations of magnetochrons (the time gap between the adjacent reversals) and the stages are substantially different: the modal duration of a magnetochron is 0.4 m.y. against the 4 m.y. modal duration of a stage. It is quite reasonable then to seek a correlation between the units which have more similar durations, such as magnetochrons and biozones. The key difficulty in this work lies in the fact that, in contrast to the scale of stages, no common geochronological stratification is suggested for the biozones. Without intending to develop such a scale, we attempt to construct some compilation of the data on the common boundaries of the biozones for correlating them to the geomagnetic reversals. This correlation is carried out in the present paper.

THE METHODS OF COLLECTING AND ANALYZING THE DATA

The time distributions of geomagnetic reversals were analyzed using the magnetochronostratigraphic scale for the Phanerozoic (Table 1) based on the collection of data presented in (Guzhikov, 2004; Molostovskii, Pechersky, and Frolov, 2007; Pechersky, Lyubushin, and Sharonova, 2010; Khramov and Shkatova, 2000; Pavlov and Gallet, 2005). The changes in the organics are traced against the alteration of biozones. The latter are the shortest stratigraphic units that have an almost global extension. In contrast to the geochronology of stages for which the global scale has been developed, there is no common global geochronological stratification for biozones. This is, obviously, applicable to yet shorter stratigraphic units such as subzones and horizons.

These units have a regional or local extent; thus, it is practically impossible to compile a global scheme for the changes of the subzones. Both magnetostratigraphic and biostratigraphic data contain plenty of controversial age estimates for the boundaries between stages, magnetochrons, and other units, which are given different

interpretations in the literature. Therefore, without focusing on these data, we tried to correlate the collected magnetistratigraphic and biostratigraphic results to a common geochronological scale, namely, to the Geologic Time Scale 2008 (GTS 2008) (Gradstein, Ogg, and van Kranendonk, 2008). In doing so, we confined ourselves to considering the ages from the lower boundary of the Tommotian Stage which is dated to about 531 Ma. In the opinion of many Russian scientists, this is the boundary between the Cambrian and Precambrian (Rozanov et al., 1997). In addition, there is only very scarce paleomagnetic evidence below the Tommotian.

The biostratigraphic data were collected in the following way. From the stratigraphic literature available on the Internet (see the list of references to the electronic table application, diamarmp@gmail.com), we selected the stratigraphic columns in which the biozones were linked to stages (ages). The columns of biozones are typically represented in terms of either thickness or time. In the latter case, time is estimated by different authors who use different geochronological scales. In both cases, we measured (in millimeters) the interval between the boundaries of the stage in the image of the column, and divided the duration of the corresponding stage from GTS 2008 (Gradstein, Ogg, and van Kranendonk, 2008) to the measured value in millimeters. Thus, the rate of sedimentation was assumed to be constant within the given stage in the given column. By doing so, we determined the time scale (the scale division). Then, we measured (in millimeters) the distance from the boundary of the stage to the boundary of each biozone within the given stage, which was then multiplied by the value of the time scale division unit.

As a result of this procedure, we obtained the age of each biozone. The estimates of the ages of the biozone boundaries determined for each column in such a way form a huge table which is impossible to quote in an article. These data are cast as electronic application available on request by e-mail (diamarmp@gmail.com). The data for the columns are summarized in Table 2 which includes information on the total number of columns for the given time interval, the number of synchronous (within ± 0.2 m.y.) biozones, the average age of the bases of the biozones, and the weight determined as the ratio of the number of synchronous biozones to the total number of columns of the corresponding age. Here, the biozones are referred to as synchronous if their lower boundaries coincide within ± 0.2 m.y. The set of collected data provide 4 to 13 stratigraphic columns per each interval of the Phanerozoic (Table 2). From the overall 831 boundaries of biozones in the Phanerozoic, 220 were identified in single columns, 193 boundaries were determined from two columns, and in the remaining 418 cases, synchronous biozones were present in at least three columns.

The magnetostratigraphic and biostratigraphic data were compared in two variants. One was a direct correlation of the boundaries of magnetochrons (geomagnetic reversals) to the biozones' boundaries, seeking the presence or absence of a direct link between these events, and the other was a comparison between the rate of change of these phenomena based on the data on the frequency of geomagnetic reversals and the rate of change of the biozones (number per m.y.).

Correlating global variation in geomagnetic reversals to the changes in the biota is hampered by several factors. For example, the biozones revealed in a single column are most likely to be a regional or a local feature in the evolution of the biota. The boundaries between biozones identified from different groups of fossils or from the same fossils but in different regions are not always synchronous (which is demonstrated in the electronic table). Cases are known of significant lateral variation in the age of the biostratigraphic boundary (Guzhikov, Baraboshkin, and Birbina, 2003; Pechersky and Garbuzenko, 2005; etc.). Obviously, the uncertainties in dating the boundaries of biozones may also be a source of considerable discrepancies, the more so in our case when we try to correlate the values calculated from the columns to the same time scale.

Taking this into account, we applied two approaches for comparing the rate of change of both time series. One approach is based on the data for 612 biozones, excluding the results identified in a single stratigraphic column. Another approach uses all 831 boundaries of the biozones, but each result is taken with the corresponding weight (Table 2). We determined the interval (increment) in time between the neighboring magnetochrons and biozones and/or the number of magnetochrons and biozones per unit time, i.e., the frequency of events. By Gaussian kernel-weighted averaging with a radius of 2 m.y. of both time series, the data were resampled onto a uniform grid. Procedures for converting the nonuniformly sampled time series into a time series sampled on a uniform time grid are described in detail in (Lyubushin, 2007). In order to eliminate the effects of minor variations, probable contributions of regional biozones, calculation errors, and other noise, the results were averaged over an interval as large as 9 m.y. shifted by 1 m.y.

The coherence in the rates of change of geomagnetic polarity and biozones is reflected in the Fourier power spectra and Morlet wavelet diagrams. Prior to calculating continuous wavelet transforms, the trend in each signal was eliminated by fitting the local polynomial of the third order in a moving time window with a radius of 15 counts.

In both time series, the symmetric magnitude-squared spectral coherence was estimated in order to describe the degree of frequency-dependent synchronism in the variations (probably shifted in phase and, correspondingly, in time). The magnitude-squared coherence (which can roughly be regarded as a squared coefficient of correlation) measures the fraction of

Table 1. The scale of geomagnetic reversals in the Phanerozoic

Chron, Ma		Chron, Ma		Chron, Ma		Chron, Ma		Chron, Ma		Chron, Ma		Chron, Ma		Chron, Ma	
0.78	N	11.71	R	25.45	N	50.03	R	128.1	N	151.5	R	177.9	N	260.5	R
0.91	R	11.9	N	25.84	R	50.66	N	128.13	R	151.6	N	178.7	R	260.7	N
0.97	N	12.05	R	26.01	N	51.85	R	128.2	N	152.2	R	180.4	N	261	R
1.65	R	12.34	N	26.29	R	52.08	N	128.65	R	152.4	N	182.4	R	261.5	N
1.88	N	12.68	R	26.37	N	52.13	R	128.9	N	152.8	R	185.6	N	262	R
2.06	R	12.71	N	26.44	R	52.83	N	129.1	R	152.9	N	186.3	R	263	N
2.09	N	12.79	R	27.13	N	53.15	R	129.2	N	153.1	R	188.9	N	263.5	R
2.45	R	12.84	N	27.52	R	53.2	N	129.7	R	153.2	N	199.3	R	264	N
2.91	N	13.04	R	28.07	N	53.39	R	129.95	N	153.5	R	202.3	N	264.6	R
2.98	R	13.21	N	28.12	R	53.69	N	130.8	R	153.8	N	203	R	264.8	N
3.07	N	13.4	R	28.51	N	54.05	R	130.95	N	154	R	214.2	N	265	R
3.17	R	13.64	N	29	R	54.65	N	131.1	R	154.3	N	214.9	R	265.4	N
3.4	N	13.87	R	29.29	N	57.19	R	131.3	N	154.7	R	216.5	N	279.5	R
3.87	R	14.24	N	29.35	R	57.8	N	131.8	R	155.08	N	217.9	R	280.5	N
3.99	N	14.35	R	29.58	N	58.78	R	132.3	N	155.1	R	219.1	N	305.1	R
4.12	R	14.79	N	30.42	R	59.33	N	133.4	R	155.2	N	220.4	R	305.6	N
4.26	N	14.98	R	30.77	N	61.65	R	133.95	N	155.4	R	221	N	307.4	R
4.41	R	15.07	N	30.82	R	62.17	N	134.21	R	155.6	N	222.7	R	308.2	N
4.48	N	15.23	R	31.21	N	62.94	R	134.3	N	155.8	R	224.2	N	311.5	R
4.79	R	15.35	N	31.6	R	63.78	N	135.2	R	156.05	N	225.8	R	312.2	N
5.08	N	16.27	R	32.01	N	64.16	R	135.25	N	156.1	R	236	N	315.1	R
5.69	R	16.55	N	34.26	R	64.85	N	135.6	R	156.29	N	241.3	R	315.3	N
5.96	N	16.59	R	34.44	N	65.7	R	135.8	N	156.4	R	242.9	N	315.8	R
6.04	R	16.75	N	34.5	R	68.1	N	136.05	R	156.7	N	243.4	R	316.8	N
6.33	N	16.82	R	34.82	N	68.3	R	136.2	N	156.8	R	244	N	317.3	R
6.66	R	16.99	N	36.12	R	69.6	N	136.7	R	156.96	N	245	R	317.7	N
6.79	N	17.55	R	36.32	N	72.6	R	136.9	N	157.1	R	247	N	318.3	R
7.01	R	17.84	N	36.35	R	73.1	N	137.8	R	157.2	N	247.4	R	320	N
7.1	N	18.07	R	36.54	N	73.2	R	138.3	N	157.3	R	248.9	N	321	R
7.17	R	18.09	N	36.93	R	74.4	N	139.4	R	157.6	N	249.7	R	321.5	N
7.56	N	18.5	R	37.16	N	74.8	R	140.8	N	157.85	R	249.9	N	321.8	R
7.62	R	19	N	37.31	R	74.85	N	141.8	R	158.37	N	250.1	R	321.9	N
7.66	N	19.26	R	37.58	N	75.2	R	142.05	N	160.3	R	250.2	N	322.6	R
8.02	R	20.23	N	37.63	R	79.8	N	143.6	R	160.8	N	250.8	R	323.3	N
8.29	N	20.52	R	38.01	N	81.6	R	143.7	N	161.2	R	251	N	323.9	R
8.4	R	20.74	N	38.28	R	82.2	N	144.4	R	161.4	N	251.2	R	324.6	N
8.54	N	20.97	R	39.13	N	83.2	R	144.5	N	161.6	R	252	N	325.6	R
8.78	R	21.37	N	39.2	R	88.3	N	144.7	R	161.7	N	253.5	R	326.7	N
8.83	N	21.6	R	39.39	N	88.7	R	145.3	N	162.2	R	254	N	330.7	R
8.91	R	21.75	N	39.45	R	107.1	N	145.8	R	162.3	N	254.5	R	331.6	N
9.09	N	21.93	R	39.77	N	108.1	R	146.1	N	162.7	R	254.7	N	332.4	R
9.14	R	22.03	N	39.94	R	109.1	N	146.2	R	164.1	N	254.9	R	333.2	N
9.48	N	22.23	R	40.36	N	110.2	R	146.6	N	164.7	R	255	N	333.6	R
9.49	R	22.6	N	40.43	R	116.1	N	147.4	R	165.3	N	255.2	R	333.9	N
9.8	N	22.9	R	40.83	N	116.3	R	147.8	N	166.6	R	255.5	N	334.2	R
9.83	R	23.05	N	40.9	R	119.7	N	149.2	R	167.7	N	256	R	335	N
10.13	N	23.25	R	41.31	N	120.7	R	149.8	N	168.8	R	256.5	N	335.3	R
10.15	R	23.38	N	42.14	R	123.6	N	149.95	R	169.2	N	257	R	335.9	N
10.43	N	24.62	R	42.57	N	124.2	R	150.05	N	169.7	R	257.5	N	338.9	R
10.57	R	24.77	N	43.13	R	124.8	N	150.7	R	171	N	258	R	344	N
10.63	N	25.01	R	44.57	N	126.8	R	150.8	N	171.7	R	258.5	N	345.9	R
11.11	R	25.11	N	47.01	R	127.5	N	151	R	172.8	N	259.5	R	347	N
11.18	N	25.17	R	48.51	N	128.05	R	151.3	N	176	R	260	N	356	R

Table 1. (Contd.)

Chron, Ma		Chron, Ma		Chron, Ma		Chron, Ma		Chron, Ma		Chron, Ma		Chron, Ma		Chron, Ma	
359.5	N	394.2	N	414.2	N	454.9	N	490.25	N	503.7	N	510.45	N	524.8	N
360.8	R	396.6	R	416	R	455.6	R	490.8	R	504.08	R	510.6	R	524.9	R
361.2	N	399	N	417.2	N	456.5	N	491.3	N	504.1	N	510.8	N	525	N
363.5	R	402.5	R	419.1	R	457.2	R	491.8	R	504.2	R	511.2	R	525.3	R
363.8	N	404	N	420.4	N	457.6	N	491.9	N	504.3	N	511.3	N	526	N
365.6	R	405.3	R	420.9	R	458.1	R	492	R	504.35	R	512	R	526.05	R
366.9	N	405.7	N	422	N	458.7	N	492.1	N	504.4	N	512.05	N	527.2	N
369.2	R	406.8	R	424.2	R	459.2	R	494.6	R	504.6	R	512.1	R	527.3	R
371.5	N	409.1	N	425.8	N	459.5	N	494.8	N	504.65	N	512.35	N	528	N
374.8	R	409.7	R	428.3	R	460.9	R	496	R	504.7	R	512.4	R	528.6	R
376.3	N	410	N	428.8	N	461.1	N	496.2	N	504.85	N	512.48	N	528.65	N
377.7	R	410.1	R	429.3	R	461.12	R	496.25	R	504.9	R	512.6	R	528.8	R
378.4	N	410.2	N	429.5	N	461.2	N	496.3	N	505.05	N	512.9	N	529	N
379.2	R	410.4	R	429.7	R	461.22	R	496.4	R	505.28	R	513	R	529.6	R
380	N	410.6	N	430.1	N	461.25	N	497.4	N	505.95	N	513.2	N	529.65	N
380.8	R	410.7	R	430.8	R	462	R	498.1	R	506	R	513.5	R	530.3	R
384.1	N	410.9	N	433.2	N	462.07	N	498.5	N	506.36	N	514	N	530.6	N
384.9	R	411.1	R	434.4	R	483.6	R	499.5	R	506.7	R	516.5	R	530.7	R
385.9	N	411.3	N	436.8	N	484.4	N	501	N	508.14	N	517.3	N	530.72	N
386.6	R	412.7	R	437.7	R	484.65	R	501.56	R	508.25	R	517.4	R	530.75	R
386.9	N	412.9	N	439.3	N	487.8	N	501.7	N	508.3	N	517.7	N	530.9	N
387.8	R	413.1	R	439.7	R	488.28	R	501.72	R	508.83	R	524.4	R		
388.7	N	413.2	N	440.8	N	488.6	N	501.8	N	509.25	N	524.43	N		
390.8	R	413.4	R	442.7	R	488.8	R	502.93	R	509.45	R	524.45	R		
392	N	413.5	N	443.5	N	489	N	503.19	N	509.6	N	524.5	N		
392.6	R	413.7	R	445.5	R	489.2	R	503.29	R	510	R	524.55	R		
393.1	N	413.9	N	448.6	N	489.3	N	503.54	N	510.2	N	524.6	N		
393.9	R	414.1	R	453.8	R	489.8	R	503.6	R	510.3	R	524.7	R		

power of oscillations in a given frequency bin, which is contributed by the linear relationship between the considered data series. This estimation is carried out with the aid of the classical method for averaging the periodograms and cross-periodograms (Brillinger, 1975; Lyubushin, 2007). After padding zeros to the length (which should be the nearest power of 2 for the Fast Fourier Transform (FFT) to be applicable), the periodograms and cross-periodograms contain 128 orthogonal frequencies.

Before padding zeros and taking the Fourier transform, we passed to the time series for increments, in order to suppress the low-frequency distortions of FFT on a finite sample and, thus, to mitigate its cyclic edge effects. Since the transition to increments is equivalent to nondegenerate linear filtering applied in a similar way to both series, this procedure, formally, does not affect the spectral coherence. After this, the periodograms and cross periodograms were averaged within a moving frequency window with a radius of 5 frequency values. The data on the ages of the magmatic activity associated with the lower-mantle plumes were taken from (Grachev, 2000; 2003; Ernst and Buchan, 2003).

THE RESULTS OF ANALYSIS

Each of the analyzed series forms a unimodal pattern with close to lognormal distribution (Fig. 1). In the case of biozones, the latter fact indicates the unity of biozones durations for different groups of organisms (Fig. 1b). In the case of magnetochrons (Fig. 1a), the histogram is incomplete due to insufficient resolution. This distribution should have been largely contributed by micromagnetochrons and excursions shorter than 0.05 m.y.

If there indeed is a direct correlation between the state of particular populations and the biosphere overall, on one hand, and the geomagnetic field, on the other hand, we should see it when directly contrasting the data on geomagnetic reversals against the changes in the organics (Fig. 2). The data in this figure have a wide scatter of values. From a total of 831 biozones in the Phanerozoic (Table 2, Fig. 2), their boundaries coincide with the geomagnetic reversals only in 52 cases. It is worth recalling that the synchronous zones here are understood as those whose boundaries are concurrent within ± 0.2 m.y. Therefore, the number of "real" (exact) coincidences is far less. The boundaries of other biozones often are close to geomagnetic reversals (Fig. 2). This similarity in ages is quite natural, as these episodes of changes of the biozones fall in the periods of

Table 2. The ages of the boundaries of biozones in the Phanerozoic

Boundary	N	No. of columns	Weight	Boundary	N	No. of columns	Weight	Boundary	N	No. of columns	Weight	Boundary	N	No. of columns	Weight
0.2	1	6	0.17	22.5	3	7	0.4	57.75	2	6	0.33	85.4	1	11	0.09
0.46	5	5	1	22.8	1	7	0.1	58.1	2	6	0.33	85.8	5	11	0.45
0.8	3	6	0.5	23.05	6	7	0.9	58.5	1	6	0.17	86.1	1	11	0.09
1.8	5	7	0.71	23.5	1	6	0.2	59	3	6	0.5	86.4	2	11	0.18
2	3	7	0.43	26.6	2	6	0.3	59.7	2	6	0.33	87.2	3	11	0.27
2.34	5	7	0.71	27.25	2	6	0.3	60.1	4	6	0.67	87.5	2	11	0.18
2.6	3	7	0.43	27.6	1	6	0.2	60.7	3	6	0.5	88.1	2	11	0.18
2.85	2	7	0.38	28	1	6	0.2	61.1	7	8	0.88	88.55	3	11	0.27
3	3	7	0.43	28.45	5	6	0.8	61.3	1	5	0.2	89	3	11	0.27
3.3	3	7	0.43	29.3	4	6	0.7	61.7	1	5	0.2	89.5	3	11	0.27
3.55	2	7	0.38	30.3	4	6	0.7	61.95	2	5	0.4	90	1	11	0.09
3.8	4	7	0.57	30.6	1	6	0.2	62.8	1	5	0.2	91.1	6	11	0.55
4.33	6	8	0.75	31.45	2	6	0.3	63	1	5	0.2	91.85	2	11	0.18
4.9	2	8	0.25	32	3	6	0.5	63.2	3	5	0.6	92.5	1	11	0.09
5.2	4	8	0.5	32.55	2	6	0.3	63.5	2	5	0.4	92.9	6	11	0.55
5.6	6	8	0.75	33.5	2	6	0.3	63.8	3	6	0.5	93.6	4	10	0.4
6	2	8	0.25	33.9	4	5	0.8	64.5	3	6	0.5	94	6	9	0.67
6.8	2	8	0.25	34	3	5	0.6	64.7	2	6	0.33	95.75	2	9	0.22
7	3	8	0.38	35	3	5	0.6	64.95	2	6	0.33	96.35	4	10	0.4
8.1	4	8	0.5	36	1	5	0.2	65.2	3	5	0.6	96.7	1	10	0.1
8.5	3	8	0.38	36.4	1	5	0.2	65.5	#	13	1	97.25	2	10	0.2
8.8	2	8	0.25	37.9	3	5	0.6	65.9	3	11	0.27	97.6	2	11	0.18
9	2	8	0.25	38.3	2	5	0.4	66.3	2	11	0.18	98.1	2	11	0.18
9.35	3	8	0.38	39.3	2	5	0.4	66.8	4	13	0.3	99.6	#	13	0.85
9.9	3	8	0.38	39.6	3	5	0.6	67.1	2	12	0.17	100.6	3	10	0.3
10.3	3	8	0.38	40	1	5	0.2	67.4	3	12	0.25	101.1	4	11	0.36
10.6	4	8	0.5	40.5	1	5	0.2	67.75	2	12	0.17	102.35	2	11	0.18
11.06	5	8	0.56	41.4	1	5	0.2	68.1	5	12	0.42	102.7	2	11	0.18
11.35	4	9	0.44	42.55	2	5	0.4	68.55	2	12	0.17	103	4	11	0.36
11.5	4	9	0.44	43.1	1	5	0.2	69	4	12	0.33	104.1	1	10	0.1
11.7	4	9	0.44	43.8	3	5	0.6	69.6	3	12	0.25	105.2	3	9	0.33
11.8	7	10	0.7	44.9	2	5	0.4	70	1	12	0.08	105.6	1	9	0.11
12.3	4	10	0.4	45.95	2	5	0.4	70.6	7	14	0.5	106	1	9	0.11
12.9	7	10	0.7	46.4	1	5	0.2	71.2	2	13	0.15	106.8	2	9	0.22
13.25	5	10	0.5	47.1	1	5	0.2	71.45	2	13	0.15	108.6	1	9	0.11
13.6	5	10	0.5	48.1	1	5	0.2	72.05	2	13	0.15	109.05	2	9	0.22
14.1	3	10	0.3	48.5	1	5	0.2	72.3	3	13	0.23	109.6	1	8	0.12
14.45	5	10	0.5	49	2	5	0.4	73	3	13	0.23	110.3	2	8	0.25
14.8	6	10	0.6	49.6	1	5	0.2	73.5	5	13	0.38	110.95	3	10	0.3
15.15	4	10	0.4	50.1	4	5	0.8	74	3	13	0.23	112	8	11	0.72
15.5	2	10	0.2	50.7	5	5	1	74.35	3	13	0.23	112.5	1	9	0.11
16.2	5	9	0.56	52.25	5	5	1	75.15	3	14	0.21	112.85	2	8	0.25
16.6	7	9	0.78	53.6	1	5	0.2	76.1	5	13	0.38	113.85	2	8	0.25
17.3	4	9	0.44	54	4	5	0.8	77.7	3	13	0.23	114.5	1	9	0.11
17.65	5	9	0.56	54.5	1	6	0.2	78.6	3	13	0.23	115	3	9	0.33
18.2	1	8	0.12	55.05	2	6	0.3	79.1	1	13	0.08	115.4	1	9	0.11
18.6	4	8	0.5	55.9	5	6	0.8	80	2	13	0.15	116.05	3	9	0.33
19.1	2	8	0.25	56.2	1	6	0.2	82	3	13	0.23	117.7	3	9	0.33
19.8	1	7	0.14	56.44	5	6	0.8	82.8	1	13	0.08	118.6	2	9	0.22
20.8	3	7	0.43	56.7	2	6	0.3	83.45	#	13	0.77	119.4	3	9	0.33
21.3	3	7	0.43	57	5	6	0.8	83.95	4	11	0.36	120.4	1	9	0.11
22.1	1	7	0.14	57.3	2	6	0.3	85	4	11	0.36	121	5	9	0.56

Table 2. (Contd.)

Boundary	N	No. of columns	Weight	Boundary	N	No. of columns	Weight	Boundary	N	No. of columns	Weight	Boundary	N	No. of columns	Weight
122	3	9	0.3	151.3	1	9	0.1	168.1	1	9	0.1	184.7	2	8	0.25
122.6	1	9	0.1	151.5	2	9	0.2	168.2	2	9	0.2	185.3	3	8	0.38
123.1	4	9	0.4	151.85	5	9	0.6	168.3	5	9	0.6	185.7	3	8	0.38
123.8	4	9	0.4	152.1	2	9	0.2	168.4	2	9	0.2	186.3	2	8	0.25
125	6	9	0.7	152.3	3	9	0.3	168.5	1	9	0.1	186.6	2	8	0.25
125.75	2	8	0.3	152.6	4	9	0.4	168.6	1	9	0.1	186.9	6	8	0.75
126.1	1	8	0.1	153	3	9	0.3	168.8	5	9	0.6	187.2	1	8	0.12
126.85	3	8	0.4	153.45	2	9	0.2	169	3	9	0.3	187.75	4	8	0.5
127.3	1	7	0.1	153.9	5	9	0.6	169.3	1	9	0.1	188	4	8	0.5
127.9	3	7	0.4	154.2	3	9	0.3	169.6	7	9	0.8	188.2	2	8	0.25
128.3	1	7	0.1	154.5	2	9	0.2	169.9	3	9	0.3	188.4	4	8	0.5
128.9	4	7	0.6	154.85	5	9	0.6	170.2	5	9	0.6	188.6	1	8	0.12
129.6	1	5	0.2	155.55	8	9	0.9	170.45	2	9	0.2	189.3	1	8	0.12
130.1	3	5	0.6	156.1	3	8	0.4	170.7	6	9	0.7	189.6	7	9	0.78
130.9	1	4	0.3	156.5	1	8	0.1	171.1	7	9	0.8	189.9	1	9	0.11
131.3	3	4	0.8	156.95	7	8	0.9	171.6	8	9	0.9	190.05	2	9	0.22
132.1	1	4	0.3	157.35	4	8	0.5	172.1	2	9	0.2	190.8	3	9	0.33
133.1	2	4	0.5	157.75	2	8	0.3	172.6	5	9	0.6	191.2	5	9	0.56
133.9	3	5	0.6	158.2	3	8	0.4	173.2	3	9	0.3	191.5	1	9	0.11
135.7	1	5	0.2	158.6	6	8	0.8	173.9	3	9	0.3	191.7	2	9	0.22
136.1	1	5	0.2	158.9	1	8	0.1	174.35	2	9	0.2	192	6	9	0.67
136.8	1	5	0.2	159.3	3	8	0.4	174.6	2	9	0.2	192.65	2	9	0.22
137.2	1	5	0.2	159.6	3	8	0.4	174.8	4	9	0.4	192.95	2	9	0.22
138.7	1	5	0.2	159.9	2	8	0.3	175.4	1	9	0.1	193.3	5	9	0.56
140.2	1	5	0.2	160.7	4	8	0.5	175.6	8	9	0.9	193.65	2	9	0.22
140.9	1	5	0.2	161.2	6	8	0.8	175.9	1	8	0.1	194	3	9	0.33
141.3	1	5	0.2	161.8	6	8	0.8	176.4	2	8	0.3	194.3	4	9	0.44
141.6	1	5	0.2	162.4	6	8	0.8	176.55	2	8	0.3	194.8	3	9	0.33
142.2	3	5	0.6	162.9	7	9	0.8	176.85	2	8	0.3	195	1	9	0.11
143	2	5	0.4	163.3	5	9	0.6	177.1	3	8	0.4	195.2	3	9	0.33
143.5	1	5	0.2	163.5	3	9	0.3	177.5	4	8	0.5	195.5	4	9	0.44
144.2	1	5	0.2	163.65	2	9	0.2	177.6	1	8	0.1	196	1	9	0.11
144.8	5	8	0.6	163.9	1	9	0.1	177.7	1	8	0.1	196.5	7	9	0.78
145.5	12	12	1	164.1	5	9	0.6	178.1	4	8	0.5	196.85	2	9	0.22
145.95	4	10	0.4	164.3	2	9	0.2	178.3	1	8	0.1	197.2	1	9	0.11
146.1	1	10	0.1	164.55	2	9	0.2	178.4	3	8	0.4	197.4	1	9	0.11
146.3	6	10	0.6	164.7	7	9	0.8	178.8	1	8	0.1	197.6	8	10	0.8
146.85	7	10	0.7	165	2	9	0.2	179.2	4	8	0.5	197.8	1	10	0.1
147.1	5	10	0.5	165.2	6	9	0.7	179.5	1	8	0.1	198.3	2	10	0.2
147.4	5	10	0.5	165.4	1	9	0.1	180.1	2	8	0.3	198.6	8	10	0.8
147.8	7	10	0.7	165.5	4	9	0.4	180.4	3	8	0.4	199.1	1	10	0.1
148.1	3	10	0.3	165.8	2	9	0.2	180.6	5	8	0.6	199.6	16	16	1
148.3	4	10	0.4	165.9	2	9	0.2	181.2	4	8	0.5	201	1	9	0.11
148.5	5	10	0.5	166.1	6	9	0.7	181.6	3	8	0.4	201.6	3	9	0.33
148.75	2	10	0.2	166.55	6	9	0.7	181.95	2	8	0.3	202.25	4	9	0.44
149.1	8	10	0.8	166.9	4	9	0.4	182.2	1	8	0.1	203.6	9	9	1
149.4	5	10	0.5	167	2	9	0.2	182.8	5	8	0.6	204.5	3	9	0.33
149.7	5	10	0.5	167.1	1	9	0.1	183	7	8	0.9	205.1	1	9	0.11
150.05	6	10	0.6	167.4	4	9	0.4	183.45	3	8	0.4	205.45	6	9	0.67
150.5	3	10	0.3	167.5	1	9	0.1	183.7	1	8	0.1	205.95	2	8	0.25
150.8	10	11	0.9	167.7	9	9	1	184.1	4	8	0.5	206.7	6	8	0.75
151.1	3	9	0.3	167.8	1	9	0.1	184.35	2	8	0.3	207.4	5	8	0.62

Table 2. (Contd.)

Boundary	N	No. of columns	Weight	Boundary	N	No. of columns	Weight	Boundary	N	No. of columns	Weight	Boundary	N	No. of columns	Weight
207.95	2	8	0.25	247.5	5	7	0.71	304.6	1	6	0.2	354.8	3	4	0.75
208.6	3	8	0.38	248.1	6	7	0.86	305.3	3	6	0.5	358.2	4	6	0.67
209.15	3	8	0.38	248.65	2	7	0.28	306.7	2	6	0.3	358.5	1	6	0.17
210	3	8	0.38	249.05	4	7	0.57	307.2	5	7	0.7	360.5	1	6	0.17
211.15	7	8	0.88	249.6	5	7	0.71	308.3	1	6	0.2	360.85	2	6	0.33
212.1	2	8	0.25	250	6	7	0.86	308.8	3	6	0.5	361.45	2	7	0.28
212.5	1	8	0.12	250.3	3	7	0.43	309.6	3	6	0.5	362.6	2	7	0.28
213	3	8	0.38	250.6	4	7	0.57	310.6	2	5	0.4	362.9	1	7	0.14
214	6	8	0.75	251	6	7	0.86	311.3	1	5	0.2	363.4	1	7	0.14
215.1	3	8	0.38	251.6	1	4	0.25	311.7	4	7	0.6	363.9	1	7	0.14
215.8	1	8	0.12	252.3	4	5	0.8	312.2	2	7	0.3	365.4	2	7	0.28
216.5	6	8	0.75	252.9	1	5	0.2	312.5	3	7	0.4	366	1	7	0.14
217.6	3	6	0.5	253.8	5	5	1	312.9	1	7	0.1	367.2	3	7	0.42
218.65	2	6	0.33	254.6	1	5	0.2	313.3	1	7	0.1	368.6	3	7	0.42
219.1	2	6	0.33	255.4	2	5	0.4	313.8	3	7	0.4	369.7	2	7	0.28
221	3	6	0.5	256.75	2	5	0.4	316.2	5	7	0.7	371.4	1	7	0.14
221.55	2	6	0.33	257.2	1	5	0.2	316.7	1	6	0.2	372.1	1	7	0.14
222.7	2	6	0.33	257.6	2	6	0.33	317.3	3	6	0.5	372.6	1	7	0.14
223.7	3	6	0.5	258.3	1	6	0.17	318.15	5	6	0.8	374.5	3	7	0.42
224.7	1	6	0.17	259.1	1	6	0.17	319.4	1	6	0.2	374.95	2	7	0.28
225.75	3	6	0.5	260.4	5	6	0.67	320.6	3	6	0.5	377.4	2	7	0.28
226.3	1	6	0.17	261.2	1	4	0.25	321.7	4	6	0.7	378.2	1	7	0.14
226.7	2	6	0.33	262	1	4	0.25	322.5	1	6	0.2	378.8	1	7	0.14
227.4	1	6	0.17	263.1	1	4	0.25	323.3	1	6	0.2	379.9	3	6	0.5
228	2	6	0.33	264	1	4	0.25	324.3	1	6	0.2	380.5	1	6	0.17
228.7	3	6	0.5	264.5	1	4	0.25	325.25	2	6	0.3	380.9	1	6	0.17
229.6	2	5	0.4	264.9	1	4	0.25	325.7	2	6	0.3	382.3	1	6	0.17
230.4	3	5	0.6	265.8	1	4	0.25	326.4	3	6	0.5	382.8	3	6	0.5
231	4	5	0.8	268	2	4	0.5	327.4	1	4	0.3	383.7	1	6	0.17
232.1	3	5	0.6	268.8	1	4	0.25	328.3	6	7	0.9	384.3	1	6	0.17
233.2	2	5	0.4	270.6	2	4	0.5	328.6	1	6	0.2	385.3	5	6	0.83
233.8	2	5	0.4	272	1	4	0.25	331.1	3	6	0.5	386	2	6	0.33
234.6	2	5	0.4	272.7	1	4	0.25	331.8	3	6	0.5	386.5	2	6	0.33
235.45	2	5	0.4	273.3	1	4	0.25	334.2	2	6	0.3	387.3	1	6	0.17
237	4	5	0.8	274.5	2	4	0.5	335.5	3	6	0.5	389	4	6	0.67
239.2	1	5	0.2	275.6	2	4	0.5	336	1	6	0.2	390.1	3	6	0.5
240	2	5	0.4	279.4	1	4	0.25	338.1	3	6	0.5	391.1	2	6	0.33
240.3	2	5	0.4	281.5	1	4	0.25	338.7	1	6	0.2	391.8	5	7	0.71
241.3	2	5	0.4	282.2	1	4	0.25	339.4	1	6	0.2	392.05	2	6	0.33
242.1	2	5	0.4	284.4	1	4	0.25	340.4	2	6	0.3	392.3	1	6	0.17
242.6	1	5	0.2	285.1	1	4	0.25	341.3	1	6	0.2	392.5	1	6	0.17
243.05	2	5	0.4	289.3	1	4	0.25	342.2	2	6	0.3	393.6	2	6	0.33
243.35	2	5	0.4	289.5	2	5	0.4	343.4	1	6	0.2	394.2	2	6	0.33
244	3	5	0.6	294.65	4	5	0.8	344.4	1	6	0.2	395.15	2	6	0.33
244.6	1	5	0.2	296.7	1	5	0.2	345.3	3	6	0.5	396.5	3	6	0.5
245.2	2	5	0.4	299	7	7	1	345.6	1	5	0.2	396.9	2	6	0.33
245.6	1	5	0.2	300.4	4	7	0.57	346.4	1	4	0.3	397.5	4	6	0.67
245.9	5	7	0.7	301.9	1	7	0.14	349.3	3	4	0.8	398.1	1	6	0.17
246.3	3	7	0.43	302.3	1	7	0.14	351	1	4	0.3	399	2	6	0.33
246.7	4	7	0.57	303.4	3	6	0.5	352.3	1	4	0.3	400.55	2	6	0.33
247	1	7	0.14	303.9	1	6	0.17	353.65	2	4	0.5	401.7	1	6	0.17

Table 2. (Contd.)

Boundary	N	No. of columns	Weight	Boundary	N	No. of columns	Weight	Boundary	N	No. of columns	Weight	Boundary	N	No. of columns	Weight
402.65	2	6	0.33	428.9	1	9	0.11	462.2	1	8	0.12	494.9	1	9	0.11
403.3	2	6	0.33	429.3	3	9	0.33	462.6	4	8	0.5	495.3	6	9	0.67
404.6	1	6	0.17	429.7	2	9	0.22	463.5	2	8	0.25	495.8	2	9	0.22
405	1	6	0.17	430.2	5	9	0.56	463.9	1	8	0.12	496.5	7	9	0.78
406.1	1	6	0.17	430.9	3	9	0.33	464.3	3	8	0.38	497.45	5	9	0.56
406.5	1	6	0.17	431.6	2	9	0.22	465.05	2	8	0.25	497.6	1	9	0.11
407	3	6	0.5	432.05	5	9	0.56	465.8	2	8	0.25	497.9	3	9	0.33
408.2	3	6	0.5	432.6	2	9	0.22	466.1	4	9	0.44	498.1	3	9	0.33
408.7	1	6	0.17	433.1	1	9	0.11	466.9	1	9	0.2	499	8	9	0.9
409.35	2	6	0.33	433.6	2	9	0.22	467	3	9	0.33	499.3	3	10	0.3
410	2	6	0.33	434.1	7	9	0.78	467.75	4	9	0.4	500.2	6	10	0.54
410.6	1	6	0.17	435.05	2	9	0.22	468.1	8	11	0.67	500.7	4	10	0.4
411.2	4	6	0.67	436	6	9	0.67	468.7	2	11	0.18	501.3	2	10	0.2
412.1	2	6	0.33	436.6	6	9	0.67	469.6	3	11	0.33	501.55	2	10	0.2
412.85	2	6	0.33	437.2	4	9	0.44	469.9	2	11	0.18	502.2	7	10	0.7
413.1	1	6	0.17	437.8	5	9	0.56	470.35	2	11	0.18	503	3	10	0.3
413.4	1	6	0.17	438	2	9	0.22	471.2	3	11	0.33	503.4	6	10	0.6
413.7	1	6	0.17	438.4	5	8	0.62	471.8	4	11	0.36	504.5	4	10	0.4
414.1	3	6	0.5	439	7	8	0.88	472.8	4	11	0.36	505.2	5	10	0.5
414.8	1	6	0.17	440.15	4	8	0.5	473.55	2	11	0.18	505.55	2	10	0.2
415.3	3	7	0.5	441.3	2	8	0.25	473.8	3	11	0.27	505.75	2	10	0.2
416	8	10	0.8	441.7	2	8	0.25	474.4	3	11	0.27	506.4	2	10	0.2
416.5	3	8	0.38	442.5	5	8	0.62	474.8	1	11	0.09	506.75	4	10	0.4
416.85	4	6	0.67	443.2	1	8	0.12	475.25	3	11	0.27	507.2	2	10	0.2
417.45	5	6	0.83	443.7	13	13	1	475.75	2	11	0.18	507.7	2	10	0.2
417.95	2	5	0.4	444.8	3	6	0.5	476.2	3	11	0.27	508.3	5	10	0.5
418.3	2	5	0.4	445.1	1	6	0.17	476.55	4	11	0.36	509.2	5	10	0.45
418.7	6	6	1	445.8	3	7	0.43	477.3	2	11	0.18	510	7	11	0.64
419.2	6	7	0.86	447.1	1	7	0.14	477.9	1	11	0.09	510.8	1	7	0.14
419.5	4	8	0.5	448.7	3	7	0.43	478.6	8	12	0.67	511.4	1	7	0.14
420	4	8	0.5	449	2	7	0.28	479.5	1	10	0.18	512.3	2	7	0.29
420.3	5	8	0.62	449.6	1	7	0.14	480.4	4	10	0.4	512.8	2	7	0.29
420.7	4	8	0.5	450	1	7	0.14	480.9	1	10	0.09	514.2	5	7	0.71
421.3	7	8	0.88	450.4	2	7	0.25	481.55	2	10	0.2	515.6	3	7	0.43
421.8	3	8	0.38	451.2	5	7	0.71	482.05	2	10	0.27	516.6	1	7	0.14
422.3	7	8	0.88	452.15	2	7	0.29	482.45	2	10	0.2	517.4	3	7	0.43
422.9	7	9	0.78	452.7	1	7	0.14	483.45	2	10	0.2	518.7	4	7	0.57
423.5	4	9	0.44	453.6	3	7	0.43	484	2	10	0.2	520.3	1	7	0.14
424.05	5	9	0.56	454	1	7	0.14	484.4	4	10	0.36	520.65	3	7	0.43
424.4	1	9	0.11	454.6	2	7	0.29	485.95	5	10	0.5	522.2	1	7	0.14
424.7	3	9	0.33	455.6	3	7	0.43	487	1	10	0.1	522.8	1	7	0.14
425.1	7	7	1	455.85	4	8	0.5	487.8	1	11	0.09	523.8	4	7	0.57
425.6	1	8	0.12	456.6	2	8	0.22	488.3	#	17	0.94	524.5	2	7	0.29
426.2	9	9	1	457.15	2	8	0.25	489	2	9	0.22	525	2	7	0.29
426.5	5	9	0.56	457.6	3	8	0.38	489.7	5	9	0.56	525.65	2	7	0.29
426.8	5	9	0.56	458.2	3	8	0.38	490.1	2	9	0.22	526.1	1	7	0.14
427.05	6	9	0.67	458.8	1	8	0.12	490.75	4	9	0.44	527.2	4	7	0.57
427.3	1	9	0.11	459.1	1	8	0.12	491.5	3	9	0.33	528.7	3	7	0.43
427.5	6	9	0.67	459.5	1	8	0.12	491.9	5	9	0.56	529.4	3	7	0.43
427.8	5	9	0.56	460	3	8	0.38	493.1	7	9	0.78	530.1	1	4	0.25
428	3	9	0.33	460.9	6	8	0.75	493.8	3	9	0.33	531	3	3	1
428.2	9	11	0.82	461.65	2	8	0.25	494.2	3	9	0.33				

Notes: the boundary is the average age of the base of the biozone, Ma; N is the number of synchronous biozones; no. of columns is the number of columns in the particular interval of ages; weight is the ratio of the number of synchronous biozones to the number of columns of the given age.

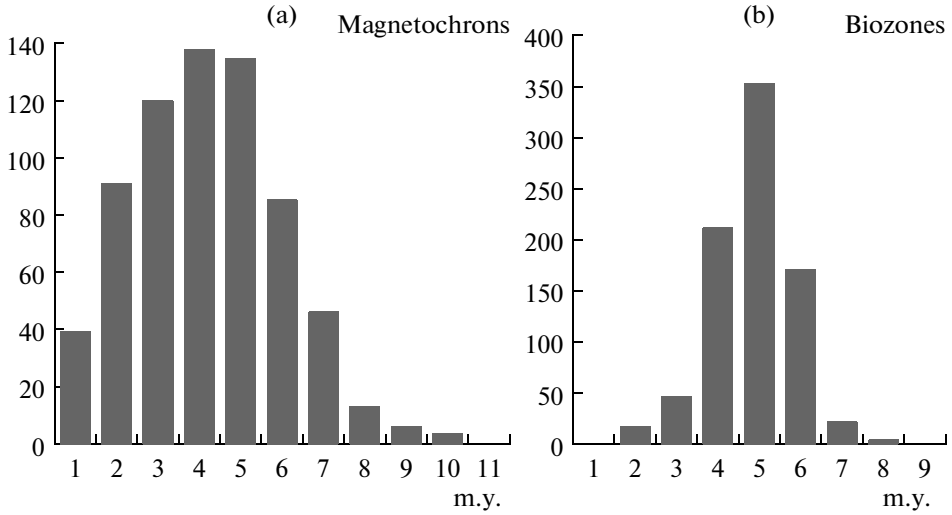

Fig. 1. The distribution histograms of durations of (a) magnetochrons and (b) biozones (based on the data from Tables 1 and 2). Time in m.y. is given on the horizontal axis: (1) 0–0.05; (2) 0.05–0.1; (3) 0.1–0.2; (4) 0.2–0.4; (5) 0.4–0.8; (6) 0.8–1.6; (7) 1.6–3.2; (8) 3.2–6.4; (9) 6.4–12.8; (10) 12.8–25.6.

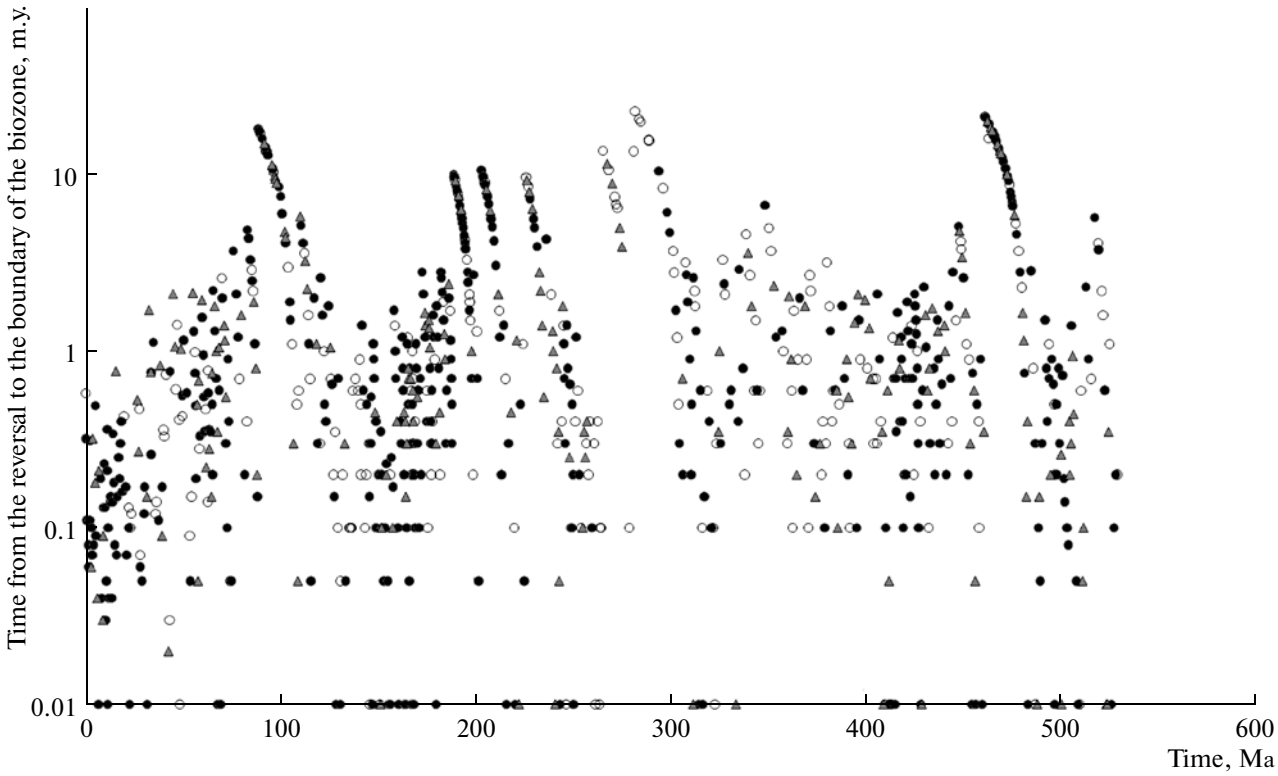

Fig. 2. Correlation of the lower boundaries of the magnetochrons with different polarity to the lower boundaries of the biozones, according to the data from Tables 1 and 2. The horizontal axis shows the age of the lower boundaries of biozones, and the vertical axis shows the difference between the nearest boundaries of the magnetochrons and biozones in m.y. The scale is logarithmic; correspondingly, the zeros are replaced with value of 0.01. The filled circles indicate the average age of boundaries of the biozones determined from at least three stratigraphic columns; these biozones likely have a global distribution. The triangles correspond to the boundaries of biozones determined from two columns. The empty circles show the ages of biozones determined from a single column; such biozones are likely of a regional spread.

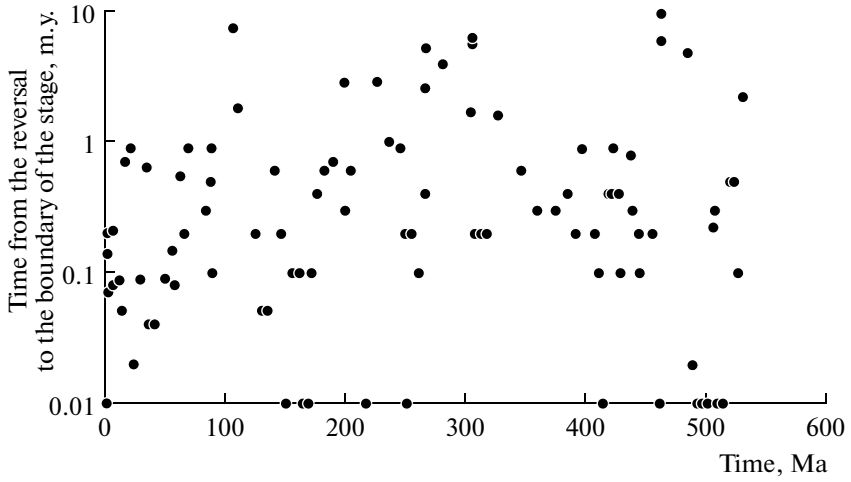

Fig. 3. Correlation of the bases of the magnetochrons with different polarities to the lower boundaries of the stages. The horizontal axis shows the age of the boundaries of the stages in Ma, and the vertical axis shows the difference between the nearest boundaries of the magnetochrons and the stages, in m.y. The scale is logarithmic; zeros are replaced with value 0.01.

frequent flips of geomagnetic polarity. The mode of magnetochron duration is about 0.4 m.y (Fig. 1); thus, the boundary of the biozone will differ from the boundaries of most of the magnetochrons by less than 0.2 m.y.

The lack of correlation between the boundaries of magnetochrons and biozones becomes more prominent when passing to the intervals with quite rare geomagnetic reversals. In these intervals, the time lags between the boundaries of biozones and magnetochrons sharply increase reaching many millions of years during the Dzhalal (85–120 Ma), Kiama (265–305 Ma), and Khadar magnetohyperchrons (460–480 Ma) (Fig. 2). Overall, in 156 cases, the mismatch between the boundaries of biozones and magnetochrons varies within 1–10 m.y. and more, and in 629 cases it ranges from 0.1 to 1 m.y. The absence of a link between the reversals and the biozones is emphasized by the almost vertical clusters of points which resemble a rocket launch (Fig. 2). This feature corresponds to the series of boundaries of biozones within prolonged time intervals of unchanged geomagnetic polarity. For example, the interval of normal polarity 89–106 Ma includes 26 changes of biozones, and 37 such changes have occurred during the interval of reversed polarity which lasted from 484 to 462 Ma.

A typical example of the absence of correlation between biota and geomagnetic reversals is the boundary between the Mesozoic and Cenozoic, which falls approximately in the middle of the C29r magnetochron with a duration of 0.85 m.y (Table 1). This is clearly traced in the sections Gubbio in Italy (Rocchia et al., 1990), Gams in Austria (Mauritsch, 1986), and Tetritskaro, Georgia (Pechersky et al., 2009).

In case of larger units, the stratigraphic stages, their boundaries coincide with geomagnetic reversals (Fig. 3) only in 13 units of the 101 units in the Phanerozoic.

In a similar manner, we have compared the times of large events, such as mass extinctions of biota (Rohde and Muller, 2005), with the polarity and reversals of a geomagnetic field (Table 3). These events were concurrent with geomagnetic reversals only in two of the ten maxima in the mass extinctions quoted in Table 3. In contrast, the boundaries of the biozones typically coincide with the peak mass extinctions (Table 3). This is not a surprise, though, because the boundaries of the biozones are, in fact, the boundaries of the creation and extinction of specific groups of organisms.

Thus, the concurrence of the boundaries of the biozones, stages, and maxima in the mass extinctions of biota with the changes of geomagnetic polarity is likely an occasional coincidence rather than a manifestation of a direct relationship between these phenomena; such a relationship seems, to all appearances, to be absent.

The presence or absence of a correlation between the processes in the core and on the surface of the Earth is traceable by the rate of change of the frequency of geomagnetic reversals and alteration of biozones. The general patterns of distribution of both data series are very similar (Figs. 4a and 4b). Coherence is more distinct in the pattern calculated for all 831 weighted biozones (Fig. 4b) rather than in the variant that excludes biozones identified in a single column (Fig. 4c) or in 1–2 columns (Fig. 4d). This may indicate that coherence is probably present in the regional features of biotic changes as well. This likeness is particularly distinct at long periods and on averaging over a larger interval (Fig. 5). The described features suggest that the processes are coherent; i.e., they probably have a common origin. However, it has been demonstrated above that a direct relationship between these phenomena is absent.

Another sign for the absence of a causal relationship between these events is the lack of a correlation (more precisely, a very weak correlation) between the change in the duration of magnetochrons and biozones. The coefficient of the correlation between these values is $r = 0.226$. Moreover, large mass extinctions in the Phaner-

Table 3. Correlation of the ages of maximal mass extinctions to the ages of the nearest geomagnetic reversals and boundaries of the biozones

Maximum, Ma	Polarity	Reversal, base	Reversal, top	Biozone, base	Biozone, top
33.9	R	34.26	32.01	33.9	33.9
65.5 (big 5)	R	65.7	64.85	65.5	65.5
145.5	R	145.8	145.3	145.5	145.5
199.6 (big 5)	N	202.3	199.3	199.6	199.6
251 (big 5)	NR	251	251	251	251
323.5	R	323.9	323.3	324.3	323.3
374.5 (big 5)	R	374.8	371.5	374.5	374.5
416	NR	416	416	416	416
443.7 (big 5)	R	445.5	443.5	443.7	443.7
518.7	N	518.9	518.5	518.7	518.7

Note: maximum is the age of peak mass extinction, Ma (Rohde and Muller, 2005); polarity is the polarity of the geomagnetic field during the peak mass extinction; N is normal polarity; R is reversed polarity; NR is the geomagnetic reversal. Reversal stands for the age of the nearest geomagnetic reversal; biozone is the age of the boundary of biozone, which is closest to the maximum extinction; base means earlier than the peak extinction; top means later than the peak extinction.

ozoic occurred during a very diverse state of geomagnetic field and do not tell on the frequency of biozones (Figs. 4a, 4b, and 6a). This fact perhaps reflects different phenomena: on one hand, natural evolution of life, which shows in the rate of change of biozones, and, on the other hand, catastrophic extinctions superimposed on the first process. A similar situation is also observed with the maxima of diversity which occurred during various geomagnetic conditions (Figs. 4a and 6b). The frequency of the alteration of biozones (Figs. 4b and 6b) exhibits a more moderate pattern: most of the diversity maxima correspond to the intervals when there were 1–2 biozones during 1 m.y.

The favorable environmental conditions which facilitated the rise of the diversity in the life forms are probably manifested in the lifetime of each of the groups of the organisms as well.

The rhythmicity of the pattern is worth noting: periods of enhanced activity in the core and on the surface of the Earth regularly and almost synchronically alternate with quiet intervals with rare geomagnetic reversals and much longer durations of biozones. A particular emphasis should be placed on the striking similarity and synchronism of the long intervals with rare reversals and rare alterations of biozones. Namely, these are the intervals of 80–120, 200–240, 270–310, 340–380, and 470–490 Ma. The likeness in the general patterns of these events, primarily, points to the coherence between the long-lasting rather than short-scale processes. The increase in the coefficient of correlation from $r = 0.226$ (averaging interval 3 m.y.) to 0.375 (averaging interval 9 m.y.) also reflects this feature.

The situation with short-scale variations in the number of the geomagnetic reversals and the frequency of the biozone alterations is much worse. As seen from Fig. 4, in some cases, the peaks in both these time series coincide, while in other cases the maxima in the frequency of reversals either lag behind or precede the frequency of the biozonal changes. The probable source of these discrepancies is the uncertainty in correlating the biozones to the magnetostratigraphic scale. However, the coefficient of correlation consistently increases as the time lag between the time series of geomagnetic reversals and the time series of biotic changes increases by 3–8 m.y.; after this, the coefficient of correlation decreases as the time lag further increases (Table 4). In other words, a tendency of the change rate of the frequency of geomagnetic reversals insignificantly lagging the frequency of biozonal changes by 6 m.y. starts to appear.

The coherence in the rate of change of the geomagnetic reversals and biozonal alterations is reflected in the power spectra of these data (Fig. 7), which contain a number of frequency components, some of which coincide or are very similar, namely, the periods of 16, 20, ~30, ~50, 60–70, and 90–100 m.y. (Fig. 7). The dark cloud on the wavelet diagram (Fig. 8) reflects the main oscillations which are common in the magnetochrons and biozones. The following rhythms are recognized in the duration of the magnetochrons: a period of 90 m.y. in the interval from 500 to 50 Ma; a period of 65 m.y. in the interval 530–0 Ma; a period of 50 m.y. in the interval 400(?)–50(?) Ma; a period of 30 m.y. in the intervals 140–60 Ma and 370–230 Ma; and a period of 20 m.y. in the intervals 120–70 Ma, 230–150 Ma, and 320–260 Ma. The biozonal durations were found to contain the following rhythms: a period of 80–90 m.y. in the interval 480–0 Ma; a period of 60 m.y. in the interval 430–220 (?) Ma; a period of 50 m.y. in the interval 300 (?)–50 Ma; a period of 30 m.y. in the intervals 160–90 Ma and 400–250 (?) Ma; and a period of 20 m.y. in the intervals 160–110 Ma and 310–240 Ma. The shorter-period oscillations, which are clearly distinguished in the power spectra, are vague in the wavelet

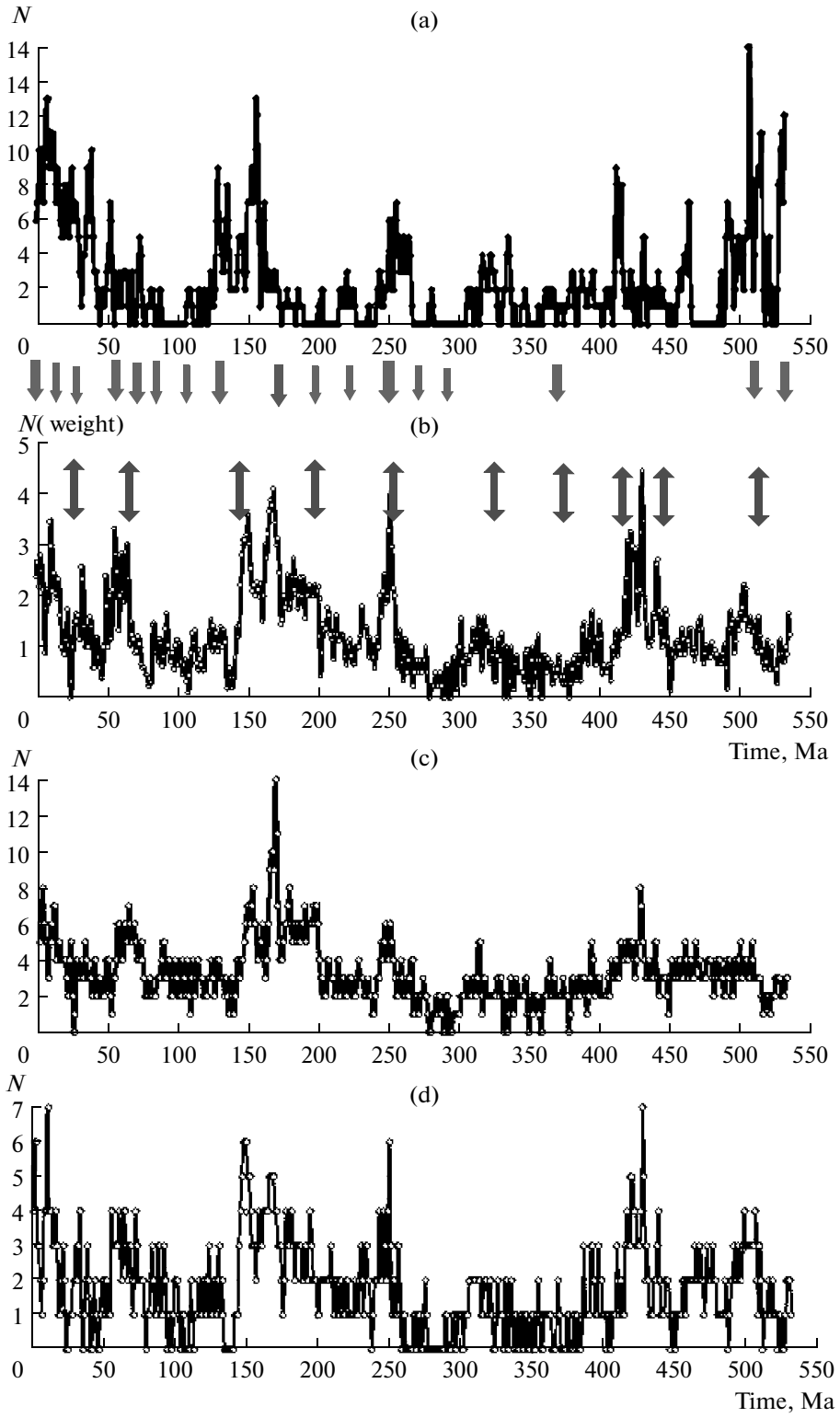

Fig. 4. Correlation of (a) the frequency of reversals to (b, c, d) the boundaries of biozones, averaging over 3 m.y. with a shift by 1 m.y. The graphs are based on the data from Tables 1 and 2, respectively. The dataset for graph 4b comprises the biozones with corresponding weights (see the text and notes to Table 2); graph 4c reflects the results with excluded biozones determined in a single stratigraphic column only; graph 4d corresponds to the data with excluded biozones identified in 1–2 columns. The vertical arrows below the horizontal axis in Fig. 4a mark the episodes of magmatism on the Earth's surface associated with the lower-mantle plume activity (Ernst and Buchan, 2003; Grachev, 2003). The arrows in the upper part of Fig. 4b indicate the maxima in the mass extinctions of biota (Raup and Sepkoski, 1982; Rohde and Muller, 2005).

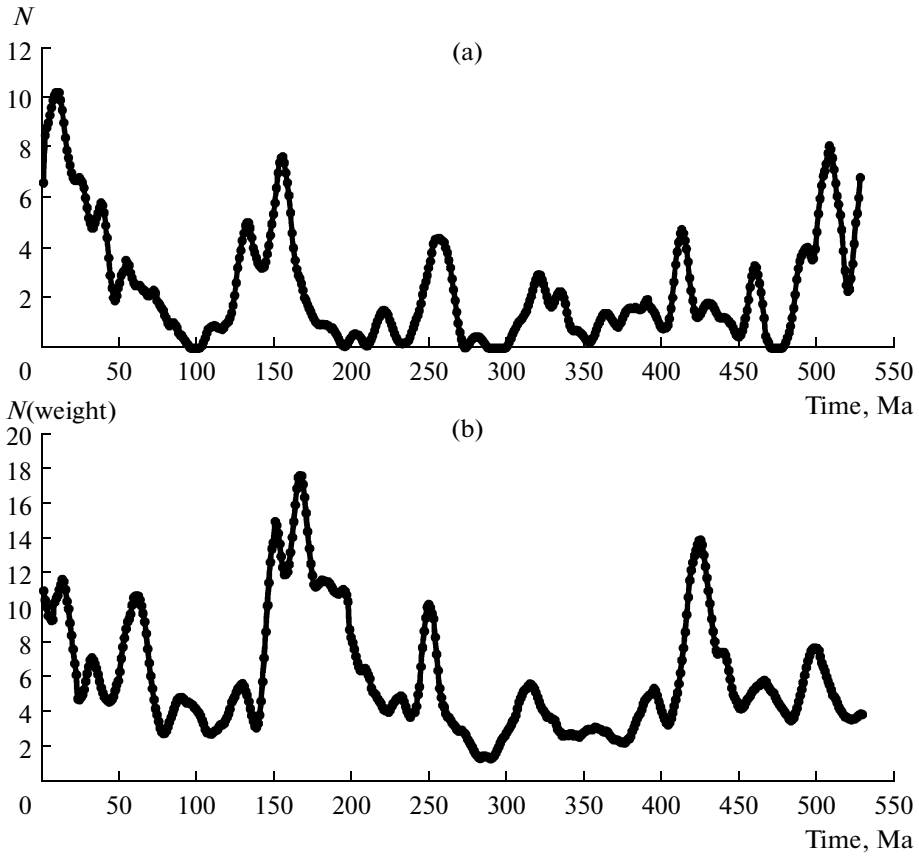

Fig. 5. Correlation of the frequency of (a) magnetochrons to the (b) biozones with averaging in a 9-m.y. window shifted by 1 m.y. Graph 5b for biozones is based on the weighted data (see the text and the notes to Table 2).

diagram where they only form some diffuse splashes. All this indicates that the series of oscillations with periods of about 50 m.y. and longer cover a large part of the Phanerozoic, whereas oscillations with periods shorter than 30 m.y. occur during relatively short intervals (Fig. 8). The likeness of the patterns for magnetochrons and biozones is remarkable.

We have figured out the degree of frequency-dependent synchronism of oscillations in both time series by estimating the symmetric magnitude-squared spectral coherence. It is seen in Fig. 9 that several periods (10, 14, 16, and 55–60 m.y.) are highly synchronous and their squared coherence is, respectively, 0.56 ($r = 0.74$), 0.59 ($r = 0.77$), 0.66 ($r = 0.81$), and 0.76 ($r = 0.87$),

Table 4. The dependence of the coefficient of linear correlation between the geomagnetic reversal and biozone scales on the time shift of the former relative to the latter

(A) averaging interval 3 m.y.									
shift	0	3	4	5	6	7	8	9	15
r	0.226	0.234	0.226	0.226	0.228	0.23	0.211	0.164	0.04
shift	0	−3	−4	−5	−6	−7	−8	−9	−10
r	0.226	0.227	0.230	0.254	0.254	0.235	0.239	0.246	0.244
(B) averaging interval 9 m.y.									
shift	0	3	4	5	6	7	8	9	15
r	0.375	0.357	0.347	0.335	0.319	0.3	0.278	0.252	0.071
shift	0	−3	−4	−5	−6	−7	−8	−9	−10
r	0.375	0.383	0.385	0.388	0.389	0.388	0.38	0.371	0.36

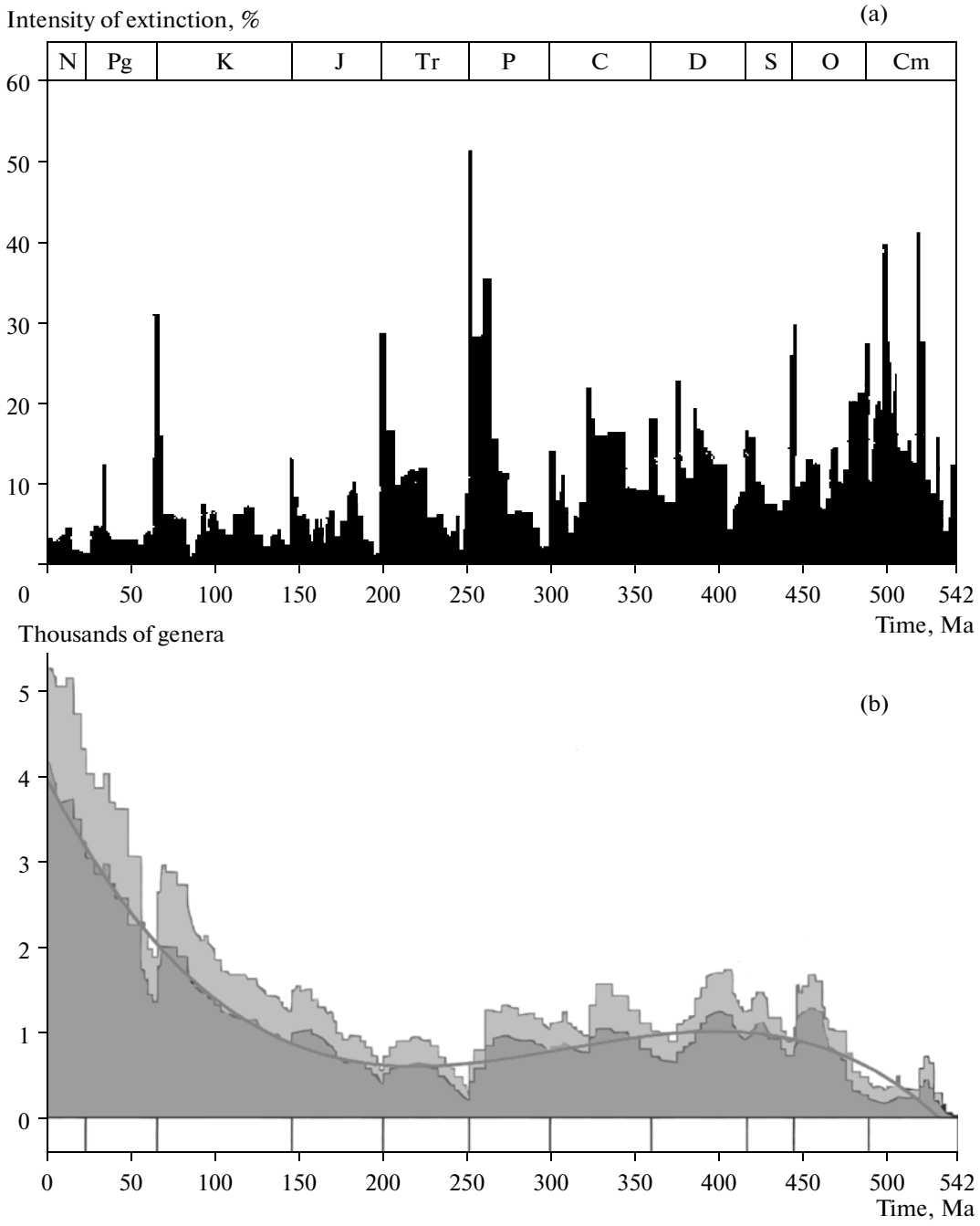

Fig. 6. The intensity of (a) mass extinctions and (b) diversity of marine organisms in the Phanerozoic (Raup and Sepkoski, 1982; Rohde and Muller, 2005).

which is far above the values typical for other periods. Here, the phase shift of the coherent oscillations ranges from zero to 10–15 m.y. of magnetochrons either lagging or preceding biozones. We recall that the phase shift by 3–8 m.y. of the time series of magnetochrons with respect to the time series of biozones is identified against an increase in the coefficient of correlation (Table 4). Obviously, in the latter case, we have the integral result contributed by all oscillations, and this result provides a more adequate view of the real situation. Even with noticeable averaging and shifting by 6 m.y., the coefficient of correlation barely attains 0.39; i.e., the probability of such shift is as small as 0.15.

Thus, on one hand, there is no correlation between the reversals (i.e., major changes in the magnitude and direction of the geomagnetic field) and the biozones (i.e., changes in the organic world). On the other hand, the rate of change of both these processes shows a distinct coherence close to synchronism. Therefore, the synchronism of the processes does not necessarily tes-

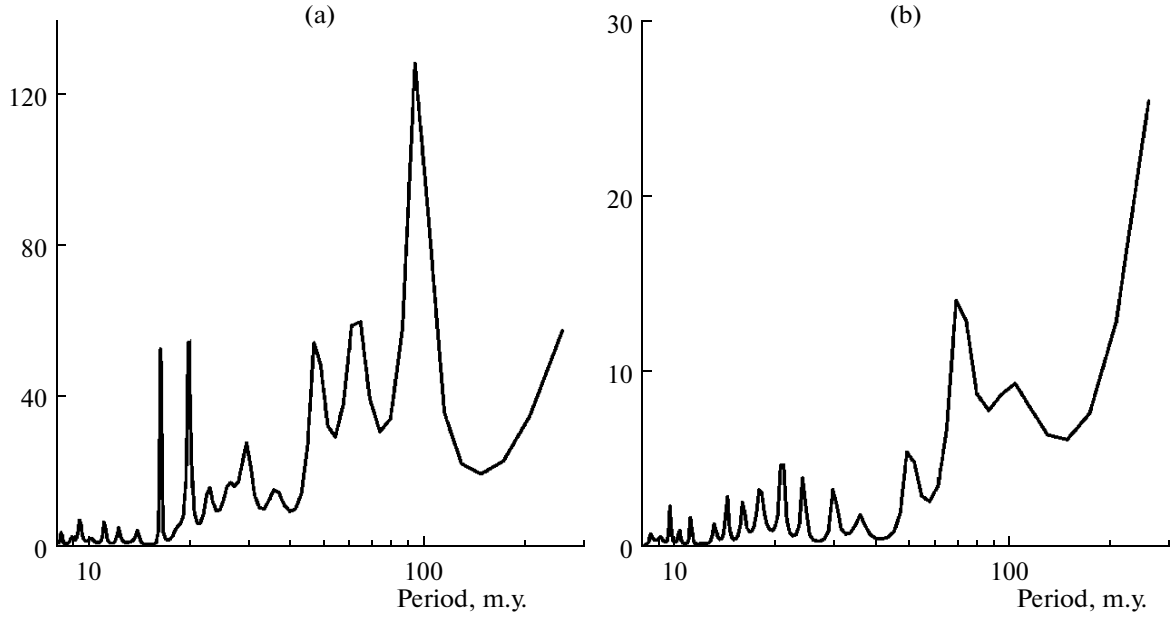

Fig. 7. The power spectral estimates for the time series of (a) magnetochrons and (b) biozones.

tify to their causal relationship. At the same time, the common source of the revealed coherent changes is quite probable. A probable common source of the coherence between the mutually independent processes originating in the core (geomagnetic reversals) and occurring on the Earth's surface (events in the biosphere) is the rotation of the Earth. The global changes in the organic world may well be due to long-lasting changes in the rotation velocity and axial tilt of the Earth. For example, it has been noticed that the onset and termination of geomagnetic excursions fall in the periods of climatic changes (Wollin et al., 1971; Bowen, 1978; Pospelova, 2000); the periods of variations in the magnitude and direction of the geomagnetic field coincide with the periods of variations in the magnetic characteristics that reflect climatic changes (Pospelova, 2000).

The Phanerozoic is clearly dominated by the reversed geomagnetic polarity (Table 1). Apparently, this reflects the fact that the Earth was always rotating in the same direction as it does today, i.e., counterclockwise. Against this background, according to the fractal analysis of the magnetochronostratigraphic scale (Pechersky, Reshetnyak, and Sokoloff, 1997; Pechersky, 2009), two regimes of generation of the geomagnetic field existed during this time. The first is the regime of frequent reversals, which is chaotic (the fractal dimension $d < 0.6$), and the second is the regime of stable field state with rare, up to no reversals, which possesses a clear self-similarity (d close to unity). The inferences of the fractal analysis are supported by the results of wavelet study: the periods shorter than 50 m.y., which are revealed in the time series of the frequency of geomagnetic reversals and the frequency of the alteration of biozones during the Phanerozoic, are relatively short events, whose time distribution appear to be rather chaotic.

We need a hypothesis that would account for the two regimes of geomagnetic field generation, on one hand, and for the coherence of processes occurring in the core and on the surface of the Earth, on the other hand. We may seek to associate both these points with the rotation of the solid inner core of the Earth relative to the mantle. For this, first, we consider nonuniformity in the Earth's rotation. There is evidence from astronomy that over the past 2700 years, the retardation of the Earth's rotation averaged 0.002 s per 100 years, and over the past 250 years, it was 0.0014 s/100 years. During the latest three decades, the rotation of the Earth is accelerating, and jumps in the rotation velocity of up to 0.004 s occur (Sidorenkov, 2004). With the average retardation assumed to be 0.002 s per 100 years, the retardation of the rotation over the entire Phanerozoic will be about 3 hours (0.002×540 Ma). This value agrees with the estimate obtained, e.g., by Munk and MacDonald (1960).

Second, it is reasonable to suppose the rotation of the inner core of the Earth to either lag or precede the mantle, depending on the acceleration or retardation of the latter, due to a liquid "gasket" between the core and the mantle, as it is theoretically demonstrated in (Groten and Molodensky, 1999). It follows from the complex of observations that the inner core is moveable and its axial rotation differs from the rotation of the whole Earth (Avsyuk, Adushkin, and Ovchinnikov, 2001). Third, it is necessary to explore the possible correlation between the geomagnetic reversals and interactions of the liquid and solid inner core of the Earth. Most

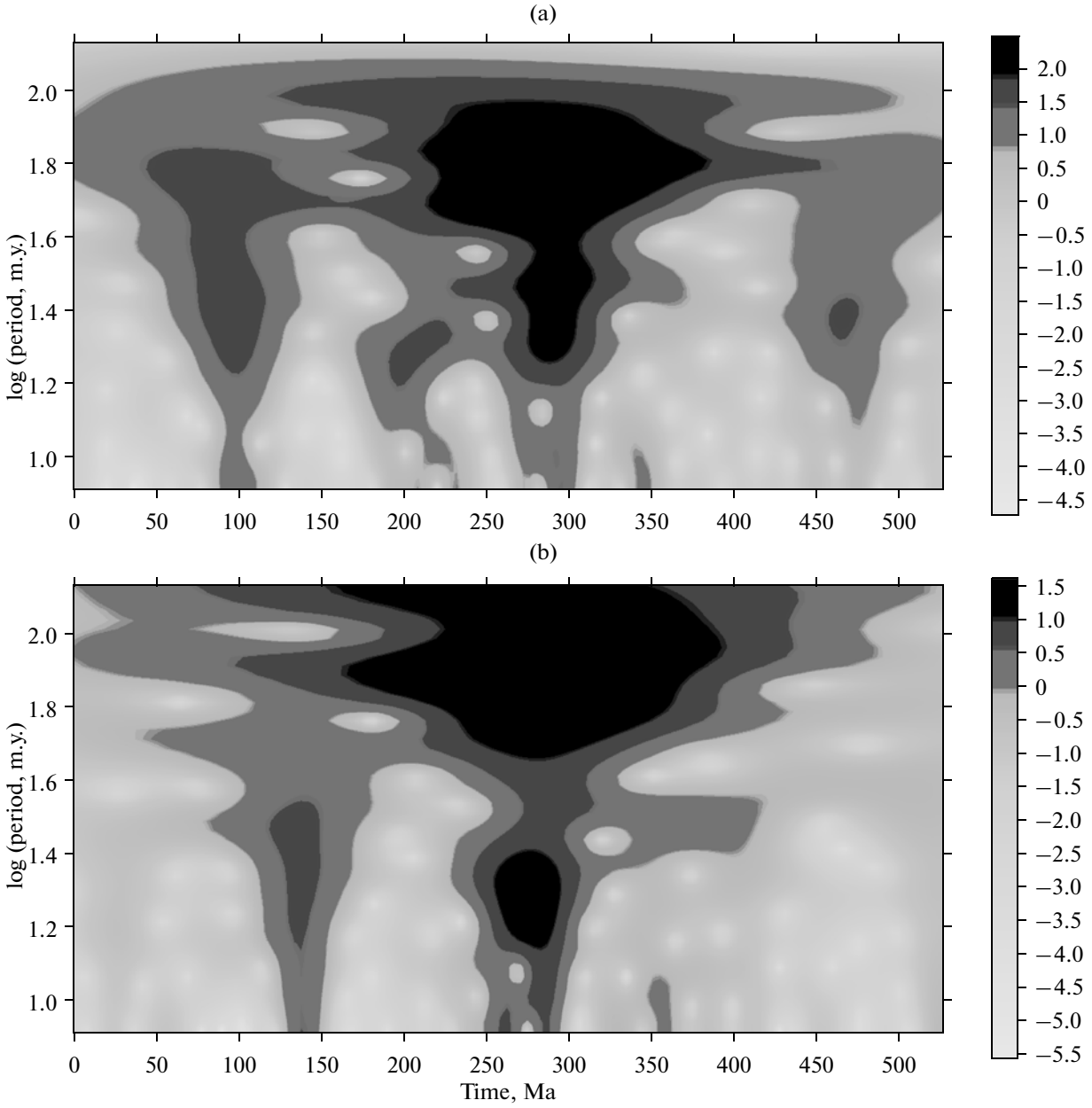

Fig. 8. The Morlet wavelet diagram for the time series of durations of the (a) magnetochrones and (b) biozones.

researchers assume a correlation of the reversals with the upper part of the liquid core that contacts the mantle. For validating this assumption, we use the data on the plumes which nucleate just at the boundary between the liquid core and the mantle (Grachev, 2000; Zharkov, Karpov, and Leont'ev, 1984; Ernst and Buchan, 2003; etc.).

In Fig. 4a, the ages of the active plume magmatism on the Earth's surface are plotted against the background pattern reflecting the frequency of geomagnetic reversals. As seen from the figure, the ages of the epicenters of plumes, as well as the times of plume formation (the age of plume magmatism plus the rise time of the plume, which is 20–50 m.y.). (Pechersky, 2001; 2007; 2009) fall in intervals of very different frequencies of geomagnetic reversals. This indicates that there is no correlation between the processes responsible for geomagnetic reversals and the formation of plumes, and, correspondingly, there is no correlation between the reversals and the phenomena in the upper part of the liquid core. It only remains to assume a correlation between the liquid outer core and the inner core.

How does the situation look in the light of our hypothesis? We believe that, as mentioned above, the

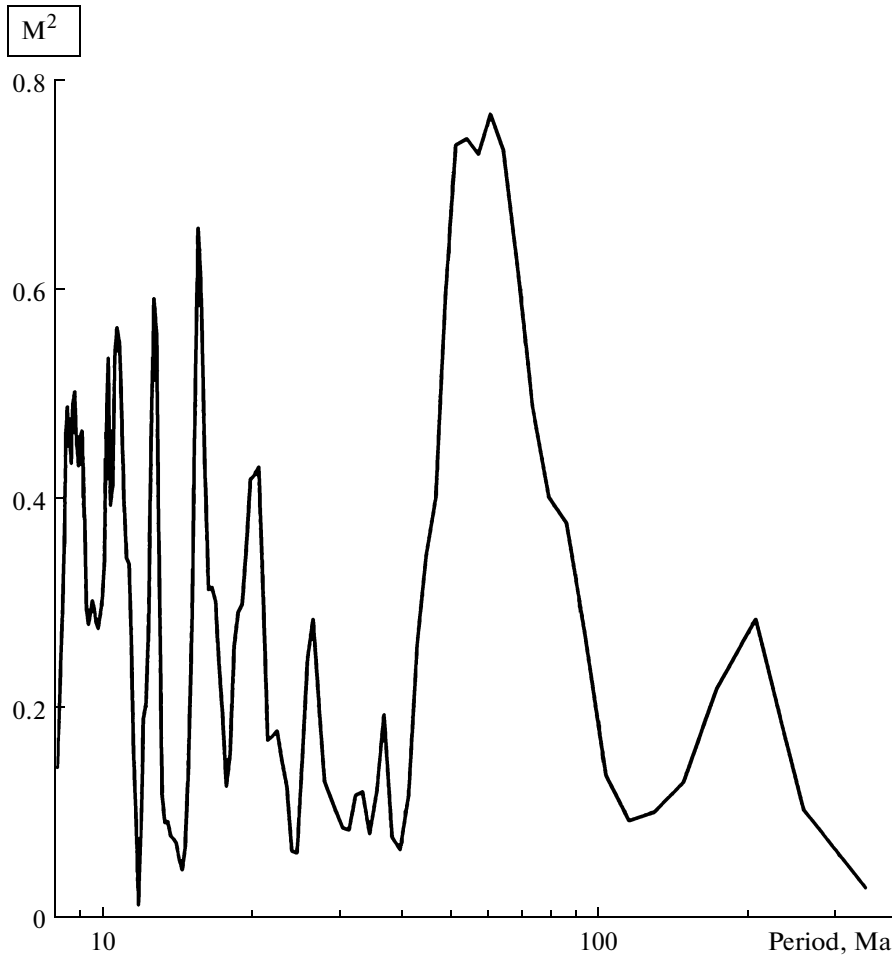

Fig. 9. The estimate of magnitude-squared spectral coherence (vertical axis, M2) between the time series of magnetochrons and biozones.

dominant reversed geomagnetic polarity is due to the counterclockwise rotation of the Earth. This polarity will persist if the inner core, the outer core, and the mantle rotate synchronously, or if the inner core precedes the remaining parts of the Earth. During the periods of acceleration of the Earth's rotation, when the inner core rotates slower than the mantle, a relative counterrotation appears at the boundary between the solid and liquid core, and, correspondingly, the field associated with this counterrotation must have the opposite sign; i.e., the same sign as the present-day field. Therefore, the long intervals of stable polarity of the geomagnetic field reflect the steady regime of the Earth's rotation. More frequently, it is a consistent retardation, which agrees with the data of astronomical, geophysical, and geological observations; far rarer, it is a stable acceleration (the Dzhalal hyperchron of normal polarity).

Both these phenomena characterize the long-period rhythm in the generation of the geomagnetic field with a period of about 180–190 m.y. (fractal dimension of about unity), likely of a galactic scale. At the same time, the intervals of frequent flips in the geomagnetic polarity relate to an unstable, close to chaotic, regime in the Earth's rotation (fractal dimension below 0.6), when retardation of the rotation frequently changes by acceleration. This regime has long lasted during the Phanerozoic. Against the background of predominantly reversed geomagnetic polarity, i.e., counterclockwise rotation of the Earth, there were intervals with unstable geomagnetic polarity: the early Paleozoic (530–483), middle Paleozoic (468–315 Ma), Mesozoic (258–123 Ma), and Cenozoic (83–0 Ma) (Table 1 (Molostovskii, Pechersky, and Frolov, 2007)). The changes in the Earth's rotation velocity should have manifested themselves in the synchronous behavior of the processes occurring on the surface and in the core of the Earth, which is what we see in our example of coherence in the frequencies of geomagnetic reversals and the changes in the boundaries of the biozones.

CONCLUSIONS

(A) From the data on the geomagnetic reversals, the biozones, the geological stages, and the maxima in the mass extinctions of the biota in the Phanerozoic, which

are cited in the present paper, it follows that a direct correlation between these events is absent. The boundaries of the geological stages, periods, ages, and biozones, and the peaks in the mass extinctions are typically not marked by changes in geomagnetic polarity. At the same time, a coherent, close to synchronous pattern of the frequency of alteration of biozones and geomagnetic polarity is observed. Synchronism of these processes is indicated by a number of common spectral components (with periods from 10 to 80–90 m.y.) revealed in these time series. The synchronism of the periods of 10, 14, 16, and 60 m.y. is quantitatively demonstrated in the changes of geomagnetic polarity and in the boundaries of biozones.

The times of plume formation correspond to the intervals with a very different frequency of geomagnetic reversals. This fact suggests that the sources of plumes and geomagnetic reversals are different. So long as the nucleation and formation of plumes is confined to the boundary between the core and the mantle of the Earth, it is reasonable to assume that the change in the sign of the field is the result of the interaction between the liquid and solid core. We suggest that the regular coherent rhythmicity in the changes of geomagnetic polarity and boundaries of biozones is associated with the variations in the rotation velocity of the inner core of the Earth and the tilt of the axis of its rotation relative to the mantle. Correspondingly, the long intervals of stable geomagnetic polarity reflect the steady regime of the Earth's rotation, whereas the intervals with frequent reversals relate to unstable rotation when retardation frequently changes to acceleration. Such a regime lasted for a long time during the Phanerozoic when it was superimposed on the background dominance of reversed polarity that corresponds to the counterclockwise rotation of the Earth.

The changes in the Earth's rotation and in the tilt of its rotational axis, which are responsible for the synchronous pattern of the change rates of the duration of magnetochrons and biozones are probably associated with the tidal evolution of the Moon-Earth system, as well as the evolution of the Earth in the solar system and in the general development of the Galaxy.

(B) To what extent is the development, evolution of living nature, due to the geomagnetic field?

The lack of a direct correlation between the changes in the biosphere with the large variations in the magnitude and direction of the geomagnetic field during the Phanerozoic, apparently, indicates that the geomagnetic field had no effect on the evolution of life on the Earth. This also follows from the fact that life on Earth has consistently progressed from the primitive unicellular forms to mammals and humans, and its diversity has grown against an approximately similar background geomagnetic field during 2.5 Ga (Shcherbakov and Sycheva, 2006; Pechersky, Zakharov, and Lyubushin, 2004) and independently of repeated reversals.

Moreover, the evolution of life was deterministic, despite the large catastrophic events in the history of the Earth. The biological clock that developed in the course of evolution has worked and keeps working perfectly: individual organisms and species are born, live, and die. There are dayflies, there are plants that live for a year, there are plants and animals that live to many hundreds of years, and this does not depend on catastrophic events—catastrophes do not break the mechanism of evolution of life once set in motion.

Thus, the evolution of life on Earth neither depends on large changes in the geomagnetic field nor on extreme catastrophic events that lead to the mass extinctions of biota. This is the main conclusion of our work.

ACKNOWLEDGMENTS

We are grateful to A.S. Alekseev, A.F. Grachev, and A.Yu. Guzhikov for carefully reading the paper and their valuable comments and recommendations.

REFERENCES

Avsyuk, Yu.N., Adushkin, V.V., and Ovchinnikov, V.M., Multidisciplinary Study of the Mobility of the Earth's Inner Core, *Izv. Phys. Earth*, 2001, vol. 37, no. 8, pp. 673–683.

Bowen, D.Q., *QuaternaryGeology: A Stratigraphic Framework for Multidisciplinary Work*,Oxford, UK: Pergamon, 1978.

Brillinger, D.R., *Time series. Data Analysis and Theory*, New York: Holt, Rinehart and Winston, 1975.

Ernst, R.E. and Buchan, K.L., Recognizing Mantle Plumes in the Geological Record, *Annu. Rev. Earth Planet. Sci.*, 2003, vol. 31, pp. 469–523.

Grachev, A.F., Mantle Plumes and Problems of Geodynamics, *Izv. Phys. Earth*, 2000, vol. 36, no. 4, pp. 263–294.

Grachev, A.F., Identification of Mantle Plumes Based on the Study of Isotopic and Geochemical Characteristics of Volcanic Rocks, *Petrology*, 2003, vol. 11, no. 6, pp. 618–654.

Gradstein, F.M., Ogg, J., and van Kranendonk, M., On the Geological Time Scale 2008, *Newslett. Stratigraphy,* 2008, vol. 43, no. 1, pp. 5–13.

Groten, E. and Molodensky, S.M., On the Mechanism of the Secular Tidal Acceleration of the Solid Inner Core and the Viscosity of the Liquid Core, *Stud. Geophys. Geodet.*, 1999, vol. 43, pp. 20–34.

Guzhikov, A.Yu., Baraboshkin, E.Yu., and Birbina, A.V., New Paleomagnetic Data for the Hauterivian-Aptian Deposits of the Middle Volga Region: a Possibility of Global Correlation and Dating of Time-Shifting of Stratigraphic Boundaries, *Rus. J. Earth Sci.*, 2003, vol. 5, no. 6, pp. 401–430.

Guzhikov, A.Yu., Paleomagnetic Scale and Magnetism of the Jurassic-Carboniferous Rocks in the Russian Plate and Adjacent Territories, *Extended Abstract of Doct. Sci. Dissertation (Geol. Mineral.),* Trofimuk Institute Of Petroleum Geology and Geophysics, Siberian Branch of the Russian Academy of Science, Novosibirsk, 2004.

Khramov, A.N. and Shkatova, V.K., General Magnetostratigraphic Scale of Polarity for the Phanerozoic, in *Dopolneniya k stratigraf. kodeksu Rossii* (Suppl. to Strati-

graphic Code of Russia), St. Petersburg: VSEGEI, 2000, pp. 34–45.

Lyubushin, A.A., *Analiz dannykh sistem geofizicheskogo i ekologicheskogo monitoringa* (Analysis of the Data from the Systems of Geophysical and Ecological Monitoring), Moscow: Nauka, 2007.

Mauritsch, H.J., Der Stand Der Palaomagnetischen Forschung in Den Ostaplen, *Leobner Hefte fur Angewandte Geophysik*, 1986, vol. 1, pp. 141–160.

Molostovskii, E.A., Pechersky, D.M., and Frolov, I.Yu., Magnetostratigraphic Timescale of the Phanerozoic and Its Description Using a Cumulative Distribution Function, *Izv. Phys. Earth*, 2007, vol. 43, no. 10, pp. 811–818.

Munk, W. and MacDonald, G.J.F., *The Rotation of the Earth: A Geophysical Discussion*, Cambridge: Cambridge Univ. Press, 1960.

Pavlov, V. and Gallet, Y., A Third Superchron during the Early Paleozoic, *Episodes*, 2005, vol. 28, no. 2, pp. 1–7.

Pechersky, D.M., Reshetnyak, M.Yu., and Sokoloff, D.D., A Fractal Analysis of the Time Scale of Geomagnetic Polarities, *Geomagn. Aeron.*, 1997, vol. 37, no. 4, pp. 490–497.

Pechersky, D.M., Neogeaen Paleomagnetism: Constraints on the Processes at the Core and Surface of the Earth, *Rus. J. Earth Sci.*, 1998, vol. 1, no. 2, pp. 103–135.

Pechersky, D.M., Changes in the Organic World and Geomagnetic Field during the Vendian–Phanerozoic, *Stratigr. Geol. Correlation*, 2000, vol. 8, no. 2, pp. 206–210.

Pechersky, D.M., The Total Amplitude of Secular Variations, Global Magnetic Anomalies and Plumes, *Izv. Phys. Earth*, 2001, vol. 37, no. 5, pp. 429–435.

Pechersky, D.M., Zakharov, V.S., and Lyubushin, A.A., Continuous Record of Geomagnetic Field Variations during Cooling of the Monchegorsk, Kivakka and Bushveld Early Proterozoic Layered Intrusions, *Rus. J. Earth Sci.*, 2004, vol. 6, no. 6, pp. 391–456.

Pechersky, D.M. and Garbuzenko, A.V., The Mesozoic-Cenozoic Boundary: Paleomagnetic Characteristic, *Rus. J. Earth Sci.,* 2005, vol. 7, no. 2, pp. 1–15.

Pechersky, D.M., The Geomagnetic Field at the Paleozoic/Mesozoic and Mesozoic/Cenozoic Boundaries and Lower Mantle Plumes, *Izv. Phys. Earth,* 2007, vol. 43, no. 10, pp. 844–854.

Pechersky, D.M., The Geomagnetic Field at the Proterozoic–Paleozoic Boundary and Lower-Mantle Plumes, *Izv. Phys. Earth*, 2009, vol. 45, no. 1, pp. 14–20.

Pechersky, D.M., Asanidze, B.Z., Nourgaliev, D.K., and Sharonova, Z.V., Petromagnetic and Paleomagnetic Characterization of Mesozoic/Cenozoic Deposits: The Tetritskaro Section (Georgia), *Izv. Phys. Earth*, 2009, vol. 45, no. 2, pp. 134–149.

Pechersky, D.M., Lyubushin, A.A., and Sharonova, Z.V., On the Synchronism in the Events within the Core and on the Surface of the Earth: the Changes in the Organic World and in the Polarity of the Geomagnetic Field in the Phanerozoic, *Izv. Phys. Earth*, 2010, vol. 46, no. 7, pp. 613–623.

Pospelova, G.A., Geomagnetic Excursions of the Brunhes Chron and Global Climate Oscillations, *Izv. Phys. Earth*, 2000, vol. 36, no. 8, pp. 619–629.

Raup, D. and Sepkoski, J., Mass Extinctions in the Marine Fossil Record, *Science*, 1982, vol. 215, pp. 1501–1503.

Rohde, R.A. and Muller, R.A., Cycles in the Fossil Diversity, *Nature*, 2005, vol. 434, pp. 209–210.

Rozanov, A.Yu., Semikhatov, M.A., Sokolov, B.S., and Khomentovskii, V.V., The Decision on the Precambrian–Cambrian Boundary Stratotype: A Breakthrough or Misleading Action?, *Stratigr. Geol. Correlation*, 1997, vol. 5, no. 1, pp. 19–28.

Roñchia, R., Boclet, D., Bonte, Ph., Jehanno, C., Chen, Y., Courtillot, V., Mary, C., and Wezel, F., The Cretaceous-Tertiary boundary at Gubbio Revisited: Vertical Extent of the Ir Anomaly, *Earth Planet. Sci. Lett.*, 1990, vol. 99, pp. 206–219.

Shcherbakov, V.P. and Sycheva, N.K., On the Variation in the Geomagnetic Dipole over the Geological History of the Earth, *Izv. Phys. Earth*, 2006, vol. 42, no. 3, pp. 201–206.

Sidorenkov, N.S., Instability of the Earth's Rotation, *Herald Russ. Acad. Sci. (Transl. of Vestn. Ross. Akad. Nauk)*, 2004, vol. 74, no. 4, pp. 402–409.

Wollin, E., Ericson, D.B., Ryan, W.B.F., and Foster, G.H., Magnetism of the Earth and Climatic Changes, *Earth Planet. Sci. Lett.*, 1971, vol. 12, no. 2, pp. 175–183.

Zharkov, V.N., Karpov, P.B., and Leont'ev, V.V., On a Thermal Regime of the Core–Mantle Boundary Layer, *Dokl. Akad. Nauk SSSR*, 1984, vol. 275, pp. 335–338.